3-10-2014

An Anomalous Near-Bottom Cross-Shelf Intrusion of Slope Water on the Southern New England Continental Shelf

D. S. Ullman
University of Rhode Island, dullman@uri.edu

D. L. Codiga
University of Rhode Island, dcodiga@uri.edu

A. Pfeiffer-Herbert

Christopher R. Kincaid
University of Rhode Island, kincaid@uri.edu

Follow this and additional works at: https://digitalcommons.uri.edu/gsofacpubs

An Anomalous Near-Bottom Cross-Shelf Intrusion of Slope Water on the Southern New England Continental Shelf

RESEARCH ARTICLE

Correspondence to:
D. S. Ullman,
dullman@mail.uri.edu

An anomalous near-bottom cross-shelf intrusion of slope water on the southern New England continental shelf

D. S. Ullman[1], D. L. Codiga[1], A. Pfeiffer-Herbert[1], and C. R. Kincaid[1]

[1]Graduate School of Oceanography, University of Rhode Island, Narragansett, Rhode Island, USA

Abstract Hydrographic surveys and moored observations in Rhode Island Sound (RIS) in water depths of 30–50 m, off the southern New England coast, revealed a near-bottom intrusion of anomalously warm and saline water in late fall 2009. The properties of this water mass, with peak salinity of nearly 35, are typical of slope water that is normally found offshore of the shelfbreak front, located approximately 100 km to the south. The slope water intrusion, with a horizontal spatial scale of about 45 km, appears to have been brought onto the outer shelf during the interaction of a Gulf Stream warm core ring with the shelfbreak east (upshelf) of RIS. The along-shelf transport rate of the intrusion can be explained as due to advection by the mean outer-shelf along-isobath current, although the transit time of the intrusion is also consistent with the self-advection of a dense bolus on a sloping shelf. The mechanism responsible for the large onshore movement of the intrusion from the outer shelf is not entirely clear, although a wind-driven upwelling circulation appeared to be responsible for its final movement into the RIS region. Depth-averaged salinity at all RIS mooring sites increased by 0.5–1 over the 3–4 week intrusion period suggesting that the intrusion mixed irreversibly, at least partially, with the ambient shelf water. The mixing of the salty intrusion over the shelf indicates that net cross-isobath fluxes of salt and other water properties have occurred.

1. Introduction

The shelfbreak front in the Mid-Atlantic Bight (MAB) separates cooler, less saline shelf water from warmer, more saline slope water and is a typical feature on buoyancy-influenced continental shelves worldwide. Although the MAB shelfbreak front is a water mass boundary, the increase in MAB shelf water salinity as it moves equatorward through the Bight [*Wright and Parker*, 1976] and salt balance calculations indicate that significant exchange across the front occurs [*Wright*, 1976]. This cross-frontal exchange is suggested by observations of parcels or streamers of shelf water offshore of the front [*Wright*, 1976; *Churchill et al.*, 1986; *Garfield and Evans*, 1987] and by observations of slope water parcels or filaments inshore of the shelfbreak. The mixing and transport of waters across the shelfbreak front has important implications for salt, nutrient, and carbon budgets on the continental shelf [e.g., *Biscaye et al.*, 1994] as well as for the recruitment of juvenile fish into coastal waters [e.g., *Hare and Cowen*, 1996]. Slope water is enriched in nitrate relative to the shelf, and mass balance calculations by *Nixon et al.* [1996] suggest that shelf-slope exchange across the shelfbreak front serves as a significant source of nitrate to the Mid-Atlantic Bight shelf ecosystem.

Incursions of slope water onto the MAB shelf have been observed in a variety of forms: as surface-intensified features [*Gawarkiewicz et al.*, 1996; *Churchill et al.*, 2003], as intrusions in the summertime pycnocline [*Boicourt and Hacker*, 1976; *Gordon and Aikman*, 1981; *Churchill*, 1985; *Lentz*, 2003; *Hopkins et al.*, 2012], and as near-bottom intrusions [*Boicourt and Hacker*, 1976; *Houghton et al.*, 1988; *Lentz et al.*, 2003; *Churchill et al.*, 2003]. The surface-intensified intrusions and the pycnocline intrusions, so-called S-max intrusions, tend to occur during the summer period of high stratification, while the near-bottom intrusions have generally been observed during fall-spring when the shelf is weakly stratified. In all of the above documented cases of near-bottom slope water intrusions in the MAB, the onshore displacement of the slope water was in the range of 10–30 km.

There is an increasing body of evidence suggesting the important influence of Gulf Stream warm core rings on exchange across the shelfbreak front. The interaction of a ring with the front has been shown to increase the susceptibility of the front to instabilities [*Ramp et al.*, 1983; *Sloan*, 1996; *Morgan*, 1997]. Modeling studies indicate the formation of a warm equatorward current of ring water along the continental slope when a ring impacts the shelfbreak [*Oey and Zhang*, 2004; *Wei and Wang*, 2009]. This process has been observed by *Wei et al.* [2008] who used repeat ship-borne current observations to show the presence of a strong (2.5 Sv)

onshore flow of ring water on the southwest side of a ring hitting the shelfbreak in the MAB. The data suggested that some portion of the onshore flow of ring water penetrated onto the shelf itself.

The onshore movement of slope water due to the movement of the shelfbreak front, whatever the cause, will result in net cross-isobath exchange only to the extent that slope water parcels mix with their surroundings before they are advected back to their original location. The inferred net onshore exchanges of salt and nitrate, referred to above, suggest that such cross-isobath exchange must happen in some manner. However, in the previous studies of near-bottom slope water intrusions over the outer shelf cited above, it was not clear that such irreversible mixing occurred.

In this paper, we present evidence for the presence of a wintertime, near-bottom intrusion of slope water as far inshore as the 40 m isobath south of New England, nearly 100 km inshore of the shelfbreak, that appeared to mix with ambient shelf water. We first examine local CTD survey data and moored observations of hydrography and currents to describe the properties of the intrusion and its progression into RIS. Shelf-wide CTD data from a NOAA survey and concurrent satellite sea-surface temperature (SST) imagery from the region are then used to suggest that the interaction of a Gulf Stream warm-core ring with the shelfbreak front resulted in the cross-frontal transport of a large slope water mass. We then discuss the question of how this slope water mass on the outer shelf could have been transported to the inner shelf of RIS.

2. Observations and Methods

The initial observations of the intrusion were obtained as part of a background investigation of the physical oceanography of Rhode Island Sound (RIS) [*Ullman and Codiga*, 2010]. A series of four hydrographic surveys of RIS and adjacent waters, using a hand-lowered CTD (SeaBird Electronics SBE 19plus), was performed at roughly 3 month intervals over a full year [*Ullman and Codiga*, 2010]. The survey grid, with stations separated by approximately 9 km was designed to cover the Rhode Island Ocean Special Area Management Plan (RI OSAMP) region, an area defined for the purpose of managing competing marine resource usages, including wind energy development. Here we discuss only the survey carried out on 7 and 8 December 2009. Although the CTD was equipped with additional sensors, we focus here only on the temperature and salinity measurements. Computation of salinity (Practical Salinity Scale) from measured temperature, pressure, and conductivity followed the standard SeaBird processing methodology, and the data were bin averaged into 1 dbar bins. Further details of the hydrographic surveys can be found in *Ullman and Codiga* [2010].

As part of the same RI OSAMP project, moored time series observations of currents were obtained at four sites (ShE, ShW, C1, and C3) in the RIS region during the fall-early winter of 2009 (shown in Figure 1). Additional current measurements were made at sites C2 and C4 as part of a separate project investigating exchange between RIS and the shelf to the southeast. The measurements at C1, C2, C3, and C4 were made using bottom-mounted acoustic Doppler current profilers (ADCP), which also provided bottom temperature, while those at ShW and ShE were made using a combination of a near-surface (2 m depth) current meter and a downward-facing ADCP. Temperature and salinity measurements were also obtained at sites C1, C3, ShW, and ShE using recording CTD instruments at various depths below a surface buoy. The moorings at C1 and C3 included seven instruments distributed from approximately 1 m below the surface to 8–9 m above the bottom. The ShW and ShE moorings were instrumented with CTDs at three depths, ranging from 1 m below the surface to 6–8 m above the bottom and also provided wind measurements from sensors mounted on the surface buoys. Details of the instrumentation and preliminary processing of the ADCP and CTD data obtained at the ShE, ShW, C1, and C3 moorings can be found in *Ullman and Codiga* [2010] (note that in this data report, stations ShE, ShW, C1, and C3 are named MD-F, MD-S, PO-S, and PO-F, respectively). Low-pass filtering of current and hydrographic time series was performed using a fourth-order Butterworth filter with a cutoff period of 36 h.

The CTD mooring strings at C1 and C3 were placed within 200 m of the ADCP bottom mounts. The string at C1 was damaged and dragged, presumably by a fishing trawler, approximately 1 km to the southwest over the course of about 2 h on 25 November 2009 (several days prior to the arrival of the deep intrusion). Although several instruments were destroyed by this impact, the instruments at depths of 28 and 35 m were unharmed and the instrument originally at a nominal depth of 7 m was moved on the wire to a depth of 3 m. All of these CTDs continued to provide good data until late December.
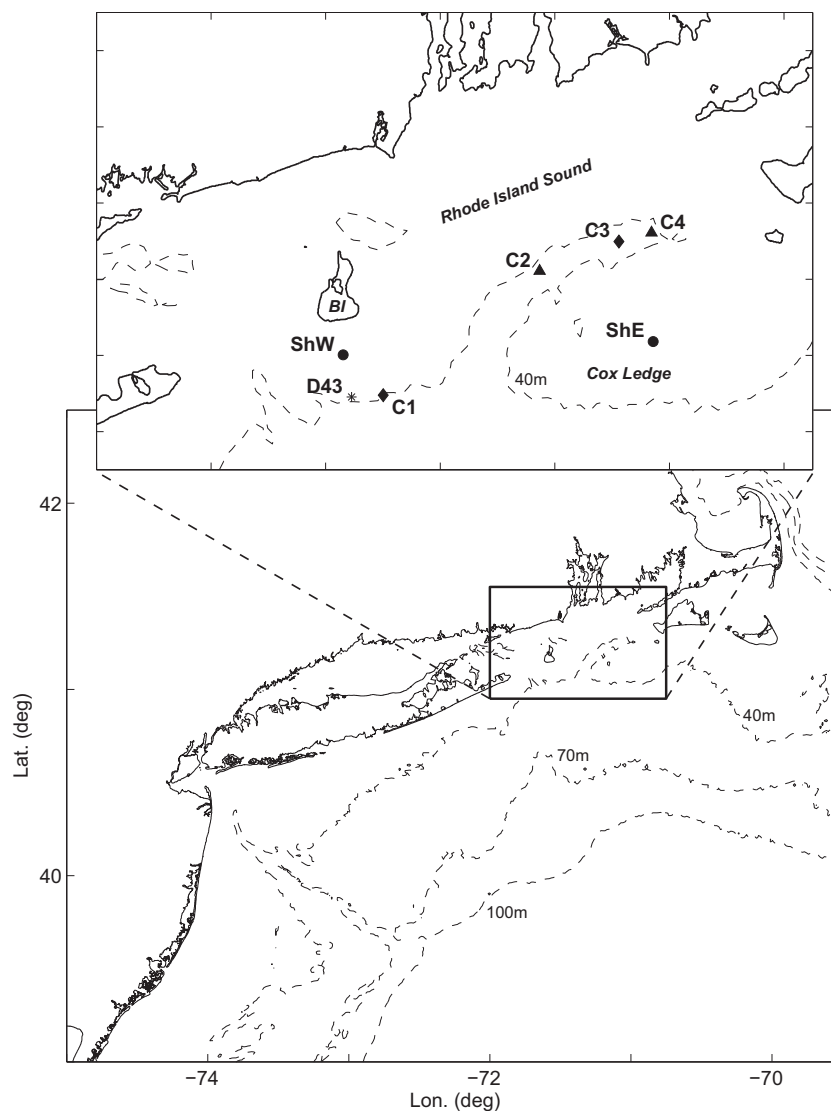
Figure 1. Southern New England shelf portion of the Middle Atlantic Bight. The inset map shows the location of the moorings in Rhode Island Sound. In the inset map, circles denote moorings that were instrumented with wind sensors, CTDs, and downward-facing ADCPs; diamonds indicate moorings instrumented with CTDs and bottom-mounted ADCPs; and triangles denote moorings with only bottom-mounted ADCPs. The star indicates the location of CTD survey cast D43 in December 2009. Geographic locations are italicized, with "*BI*" referring to Block Island.

Archived hydrocast data for the New England shelf region, covering the time period 1916–2009, were extracted from NOAA's World Ocean Database (WOD) 2009 [*Boyer et al.*, 2009]. For the region of interest (72–70°W, 39–41.5°N), there were a total of 855 casts during the months November–January, including 98 casts within 25 km of mooring site C1. We also obtained, from NOAA's Northeast Fisheries Science Center (NFSC), CTD data from a survey cruise on the MAB shelf during early November 2009.

All available SST imagery covering the southern New England shelf and slope were obtained from the Mid-Atlantic Regional Association Coastal Ocean Observing System (http://maracoos.org) for the period November–December 2009. To reduce the impact of clouds, all images from each day were combined into composite images using the warmest-pixel method [*Legeckis and Zhu*, 1997].

3. Results

3.1. Description of Intrusion

The CTD survey in December 2009 showed the presence of a near-bottom layer that was anomalously warm and saline, with temperatures above 15°C and salinities above 34 (Figure 2). Average autumn
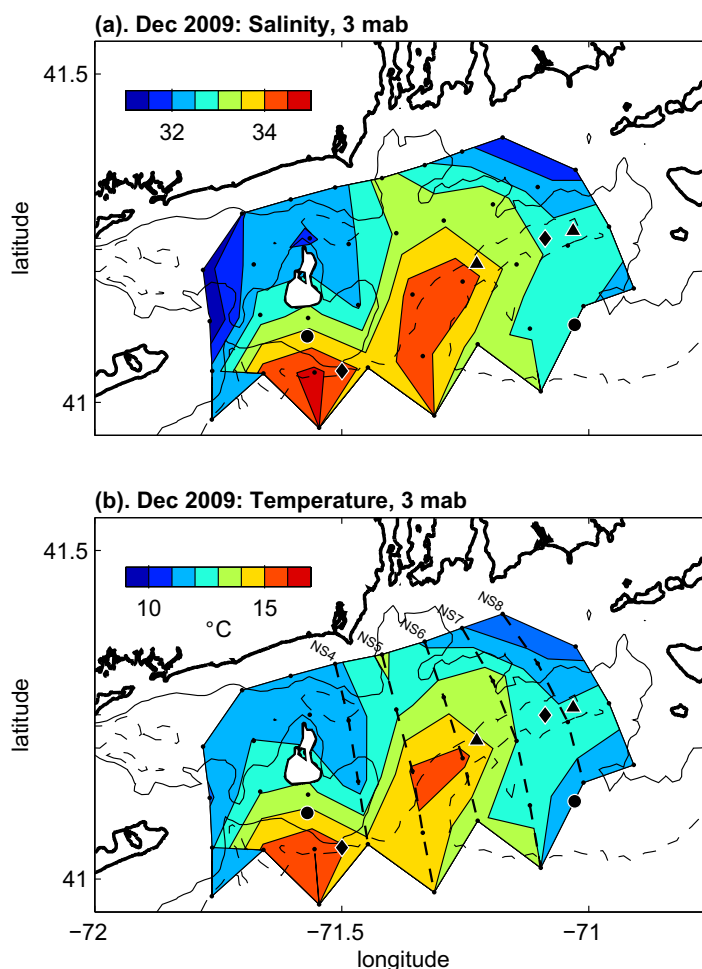
Figure 2. Maps of (a) salinity and (b) temperature at 3 m above the bottom from CTD casts on 7 and 8 December 2009. The small black dots indicate the CTD station locations. The mooring locations are denoted by the larger symbols (see Figure 1 for the site names). The 30 and 40 m isobaths are shown, respectively, by the thin solid and dashed lines. The heavy dashed lines in Figure 2b show the north-south lines along which vertical salinity sections are plotted in Figure 10.

near-bottom conditions in southern RIS, where the intrusion was observed, are temperatures from 12.5 to 13.0°C and salinities from 32.5 to 33.0 [*Codiga and Ullman*, 2010]. The intrusion extended northward (onshore) into RIS via the deep channel between Block Island and Cox Ledge (Figure 2). Although some stations along the southern boundary of the survey grid were not occupied due to operational constraints, it seems clear that the anomaly was an intrusion from offshore and was most intense directly south of Block Island. At its thickest point, along the southern edge of the survey grid, the intrusion (defined as water with salinity >33) extended to approximately 20 m above the bottom [*Ullman and Codiga*, 2010].

The warm, high salinity intrusion was detected by the deep CTD sensors at C1 (water depth 44 m), where an abrupt increase of salinity and temperature by approximately 2 salinity units and 4°C over roughly 6 h was observed at 35 m depth on 28 November 2009 (Figure 3). Subsequently, the 35 m salinity slowly increased to a maximum of ~34.5 before

decreasing again to <33. This was followed by another salinity increase to a maximum of 35 before decreasing abruptly in late December to approximately 33. From start to finish, the anomalous water was present at the mooring location for 3–4 weeks. The intrusion extended upward at times to at least 28 m depth (approximately 16 m above the bottom) with significant high frequency (tidal) variability evident in the 28 and 35 m T and S (Figure 3). Near-surface salinity at C1, while exhibiting much less variability than at depth, decreased by about 0.5 at the time of arrival of the deep intrusion and Figure 3 suggests that, during the intrusion period in general, near-surface salinity varied inversely with deep salinity.

At mooring C1, the abrupt increases in salinity and temperature at 35 m observed on 28 November and then again on 11 December (denoted by the upward arrows in Figure 3) after an intervening relaxation were accompanied by very strong, surface-intensified eastward currents with magnitudes of ~0.5 m/s (Figure 3). Velocity vectors rotated counterclockwise (onshore) with depth. Maximum onshore currents occurred at about 10 m above the bottom, with magnitudes in the range of 0.3–0.4 m/s. The deep onshore and eastward current pulses were coincident with the occurrence of strong (~15 m/s) eastward, upwelling favorable, winds (Figure 3). In contrast, the abrupt salinity and temperature drops at depth at C1, occurring on 9 and 20 December (denoted by the downward arrows in Figure 3), were accompanied by surface-intensified westward and weak offshore near-bottom currents associated with westward (downwelling favorable) winds. The sense of near-surface (7 m) salinity responses to these upwelling-favorable and
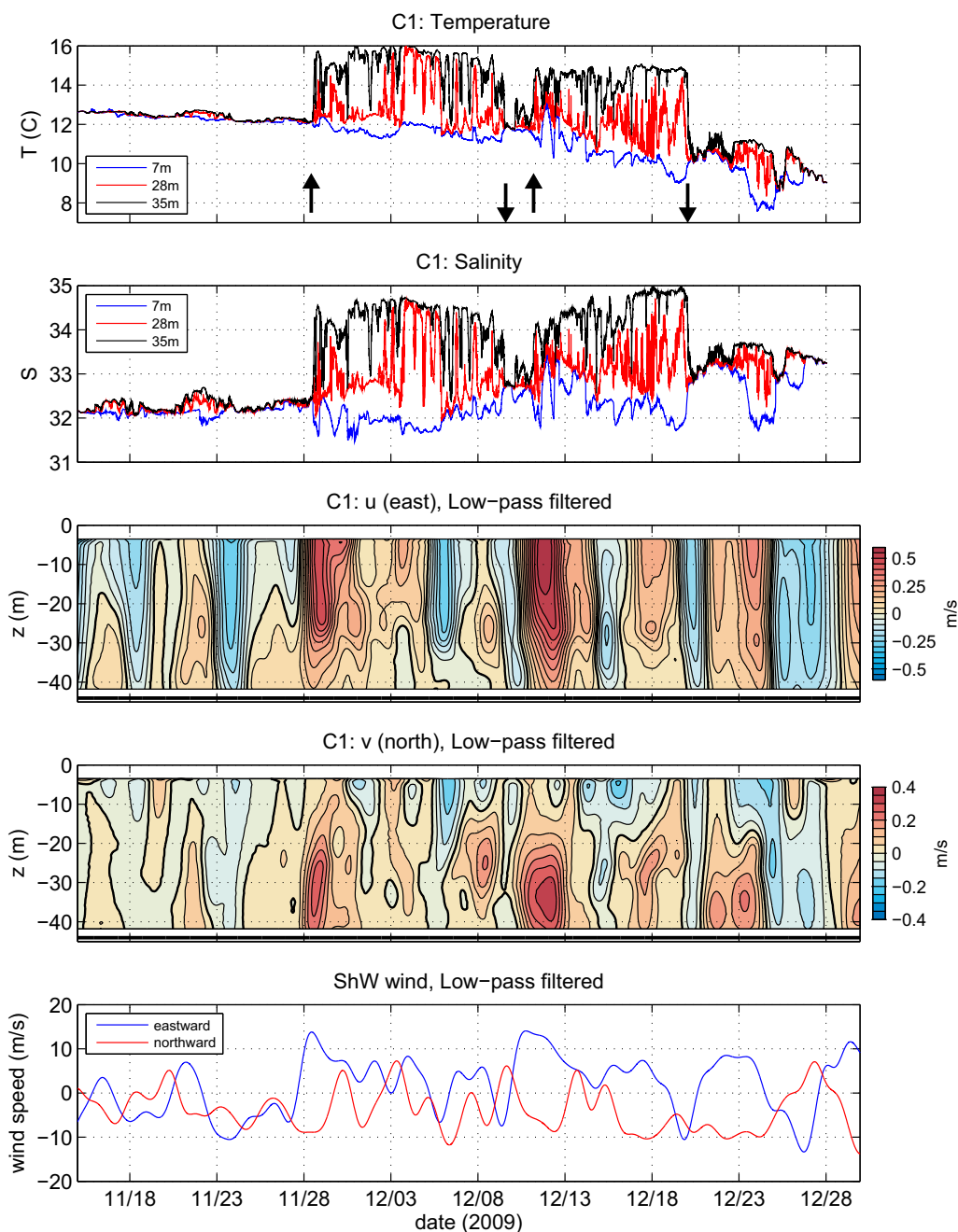
Figure 3. Mooring observations at site C1 during November–December 2009. Top to bottom are temperature and salinity from moored CTDs, low-pass filtered current in the eastward and northward directions, and low-pass filtered wind velocity in the eastward and northward directions at the nearby site ShW. The arrows in the top plot denote times of intrusion advances (up arrows) and retreats (down arrows).

downwelling-favorable wind fluctuations was, as mentioned above, opposite the near-bottom fluctuations. As this mooring is located southeast of the Long Island Sound outflow plume [*Ullman and Codiga*, 2004], this behavior is consistent with wind-driven advection of the plume past the mooring, with upwelling (downwelling) winds tending to move the plume offshore (onshore).

Although the effects on water density of the temperature and salinity changes associated with the intrusion are opposing, plotting the 35 m mooring observations from C1 on a T/S diagram (Figure 4) shows that the density of the intrusion is higher than the ambient water (preintrusion conditions of $T = 12°C$ and $S = 32$)

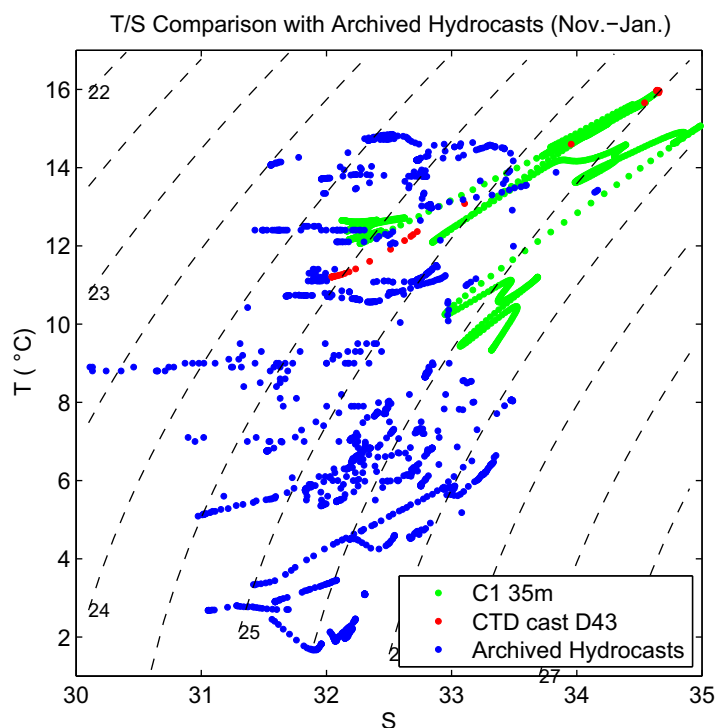T/S Comparison with Archived Hydrocasts (Nov.–Jan.)

Figure 4. Temperature versus salinity plot for all archived hydrocasts within 25 km of the C1 mooring location during the months November through January (a total of 98 casts over the period 1946–2009). The corresponding T-S characteristics at 35 m depth at mooring C1 from 15 November to 31 December 2009 (low-pass filtered and resampled to 1 h) is shown by the green points. The red points denote the CTD cast D43, obtained at a site 4.6 km from C1, on 8 December 2009. The dashed contours denote σ_t in kg/m^3.

by 1–1.5 kg/m^3. This suggests that the intrusion is not of the S-max type [*Lentz*, 2003; *Hopkins et al.*, 2012] which tend to move along isopycnals and which are observed at midwater column depths.

3.2. Comparison With Archived Observations

We examined archived hydrographic cast data to determine the degree to which the observed intrusion was anomalous. Figure 4 shows the *T/S* characteristics of all archived hydrocasts taken within 25 km of the C1 mooring location along with the data from the deep sensor on the mooring and those from the nearest CTD cast (4.6 km away), denoted D43 in Figure 1, from the December 2009 survey. Salinities from the archived casts are almost always <33.5, with only three data values from a single cast, in December 1979, >34. The observed maximum salinity of 35 at the mooring is thus roughly 1 salinity unit higher than had ever been observed in the archived data, indicating that the fall 2009 event was a rather uncommon occurrence.

Further analysis of the archived hydrocast data from the portion of the MAB shelf offshore of the C1 mooring shows that water with salinity of 35 (the maximum observed salinity at mooring C1) is exceedingly rare inside the 70 m isobath. Figure 5 shows the percentage of hydrocasts where $S > 35$ water was encountered, binned as a function of water depth (20 m bins). At water depths of 50–70 m, the percentage is <1% and the percentage only rises to slightly >9% for the 70–90 m depth bin. The percentage rises rapidly around the 100 m isobath, roughly the location of the foot of the shelfbreak front in this region. This indicates that the salinity of the intrusion water is consistent with the hypothesis that the intrusion originated in the shelfbreak front or the slope water offshore of the shelfbreak.

3.3. Spatial and Temporal Variability of Intrusion

The intrusion was also detected at the other moorings as well as at C1. Figure 6 shows low-pass filtered salinity at the four moorings where water column hydrography measurements were made during the late November–December time period. Note that although CTD measurements at seven depths are available at C3, for clarity in Figure 6 we show only three depths corresponding to the depths available at C1. Although the highest salinity jump occurred at C1, where deep salinity increased by 2–3, deep salinity at all other sites also exhibited a similar abrupt increase of >1 slightly after the increase at C1. Although the initial jump in salinity at depth is unambiguous at all sites, the temporal fluctuations in salinity that occur after the arrival of the intrusion differ from site to site. At the deep sites, C1 and C3, the 35 m salinity exhibits an approximately 2 week periodicity that appears to be related to fluctuations in the wind-driven shelf currents as seen in Figure 3. This long-period variability is also present at the shallower ShW and ShE sites but at those locations, fluctuations at shorter periods (2–5 days) appear to be more dominant. At ShE, after an initial period during which the intrusion is bottom intensified with significant vertical salinity stratification, surface
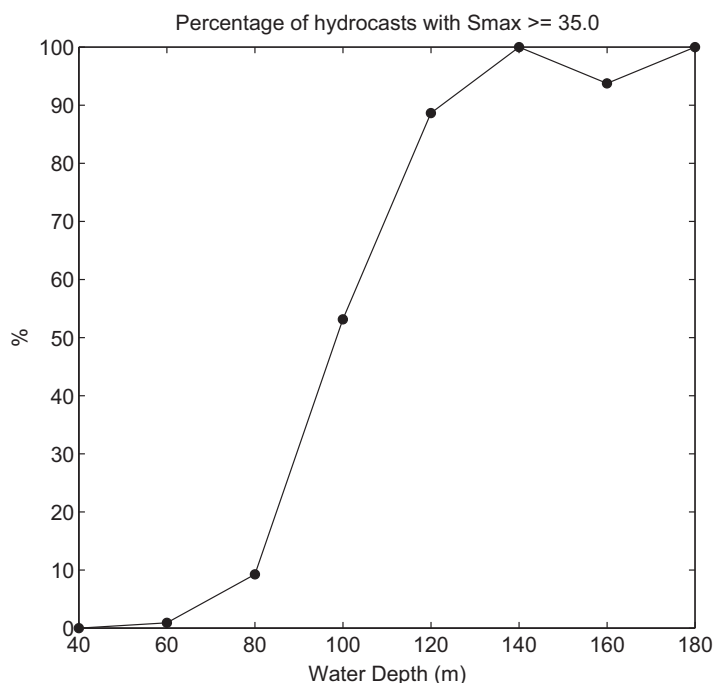
Figure 5. Percentage of archived hydrocasts detecting salinity of 35 or higher as a function of water depth for the northern MAB shelf (72–70°W, 39–41.5°N).

to bottom salinity differences are reduced to less than about 0.25 after 3 December. This occurs to a lesser extent at ShW and C3.

Bottom temperature observations from the four bottom-mounted ADCPs (sites C1–C4) show the advance of the deep intrusion along an approximate straight line extending from the shelf into RIS through the deep channel north and west of Cox Ledge (see Figure 1 for the geographic locations). Figure 7a shows that the initial temperature jump associated with the arrival of the deep intrusion occurs first at C1, followed sequentially by jumps at sites C2, C3, and C4. Temperatures at C4 and C3 decrease starting around 8 December, followed approximately 2 days later by temperature decreases at C2 and C1, suggesting a large-scale offshore retreat of the intrusion. This is followed by subsequent temperature increases, occurring in the same sequence as the initial jumps. The final temperature drop at all sites occurs in the same order as the first retreat although with substantially shorter time lags on approximately 20 December. Near-bottom subtidal currents during the initial and secondary intrusion advances (Figures 7b and 7c) are strongly eastward at all sites with magnitude of 0.15–0.25 m/s with slightly stronger northward currents observed at C1 and C2 but with nearly zero north-south current at the two interior sites (C3 and C4). Near-bottom currents are thus oriented roughly in the proper sense to advect intrusion water from C1 on the shelf into RIS via the deep channel.

The times of arrival of the initial intrusion pulse at sites C1–C4 were visually estimated from the bottom-temperature records and are shown in Figure 8a as a function of distance from site C1. The intrusion gradually slows as it proceeds northeast (Figure 8b), reaching site C4 approximately 2 days after passing C1. The propagation speed of the intrusion estimated from the time of arrival of the temperature jump slows from approximately 35 km/d between C1 and C2 to about 10 km/d between C3 and C4 (Figure 8b). These speeds are significantly faster than the speeds estimated from the measured ADCP velocities, assuming that the movement of the anomaly is due purely to advection along the line joining two sites. To estimate the advection speed, we used the ADCP velocity at 10 m above the bottom, resolved into the component in the direction of the line joining two adjacent sites. These velocities were averaged over the time between the arrival of the temperature pulse at each site and then averaged over the two adjacent sites. The estimates range from approximately 5 to 24 km/d, although they exhibit a similar decrease with distance as do the estimates from the temperature anomalies (Figure 8b). If velocities at 20 m above the bottom are used (Figure 8b), the differences between the two methods are reduced, but the ADCP velocities still underestimate the propagation speeds. The underestimate of the propagation speed using the velocity along the line joining the mooring sites suggests that the intrusion is not being advected exactly along the line. Any perpendicular advection would tend to increase the apparent propagation speed estimated from the arrival times.

We also show, in Figure 8b, the intrusion speed assuming that the intrusion propagates as a gravity current over a flat bottom (depths at all sites are approximately the same). The propagation speed was computed using the formulae in *Shin et al.* [2004] with a 20 m deep current in 40 m water depth and a 1 kg/m^3 density
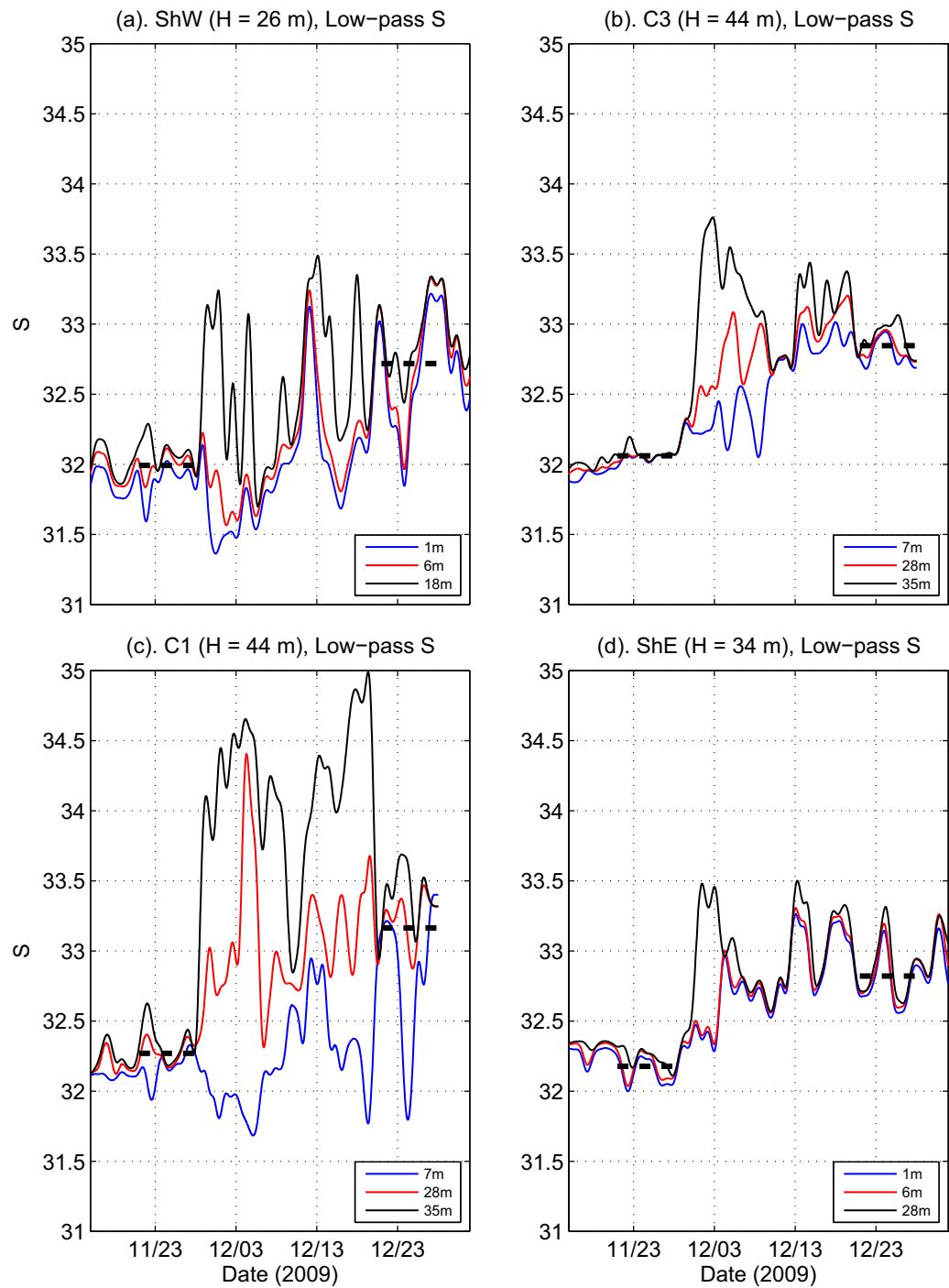
Figure 6. Low-pass filtered salinity from moored CTDs at sites (a) ShW, (b) C3, (c) C1, and (d) ShE. The heavy black dashed lines indicate the mean, depth-averaged salinity over 7 day periods prior to the arrival of and after the retreat of the intrusion.

difference. The computed gravity current speed is roughly the correct magnitude, but the gravity current model does not explain the slowing of the intrusion as it propagates to the northeast.

Progressive vector diagrams for 4 day periods prior to the time of arrival of the intrusion at the four bottom-mounted ADCP sites were constructed using hourly averaged velocities from 10 m above the bottom and a trapezoidal integration scheme (Figure 9). These pseudotrajectories, which must be viewed with caution given the underlying assumption of spatial uniformity in currents, suggest that the anomalous
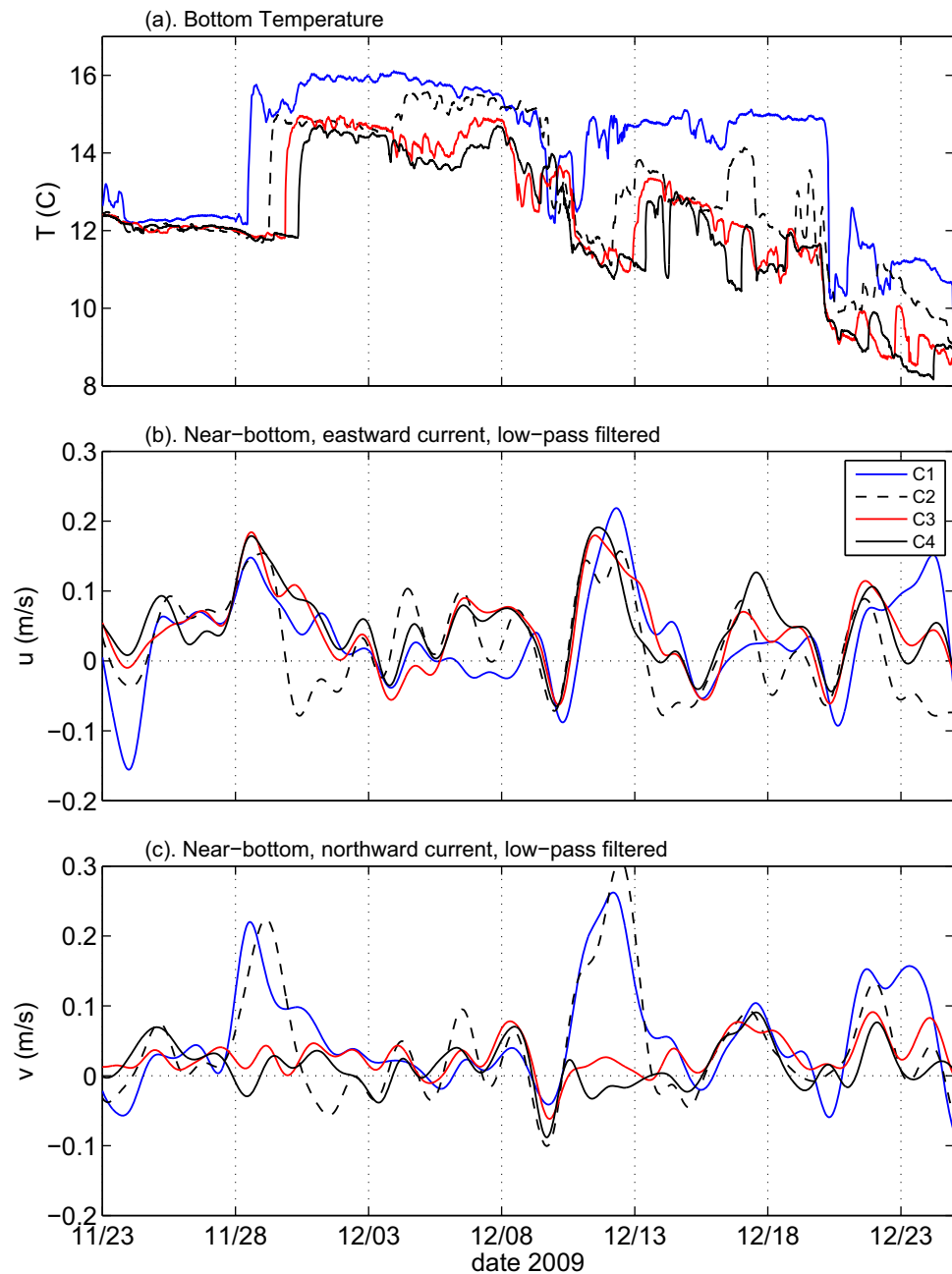
Figure 7. (a) Bottom temperature, (b) near-bottom, low-pass filtered eastward currents, and (c) near-bottom, low-pass filtered northward currents from bottom-mounted ADCPs at sites C1, C2, C3, and C4 during November–December 2009.

water reached C1 from roughly the southwest. The trajectory at C2 during the final day is more from the south. The C3 and C4 trajectories suggest advection from the west. The pseudotrajectories reinforce the above suggestion that the advection of the anomaly is not directly along the path defined by the four stations. The suggestion from Figure 9 is that the anomaly approaches C2 from a more offshore direction and then swings to the east to impact C3 and C4.

3.4. Evidence for Mixing of Intrusion

The presence of slope water on the shelf far inshore of the shelfbreak prompts investigation of the question of mixing between the intrusion water and the ambient shelf water. As noted above, Figure 6 shows that in early December 2009, vertical salinity stratification weakens significantly at sites ShE, ShW, and C3. Vertical
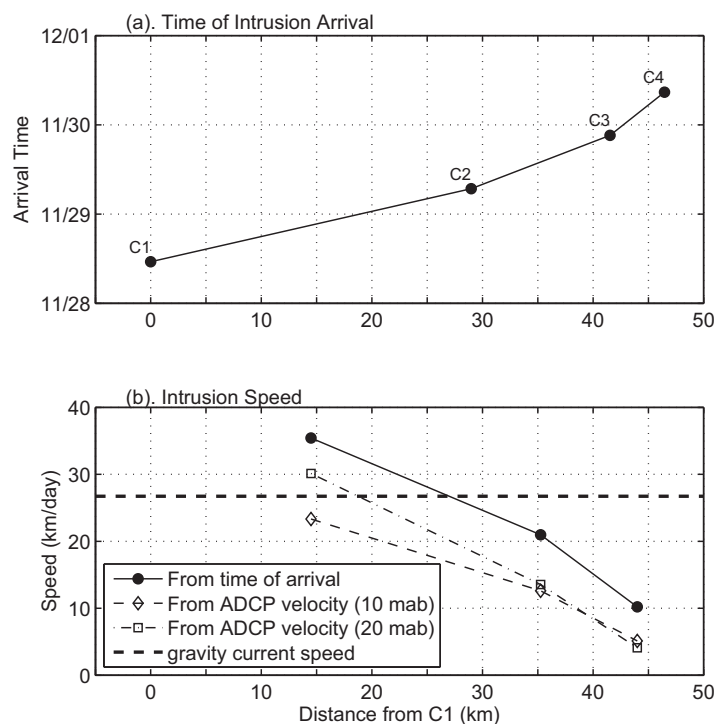
Figure 8. (a) Arrival time of high temperature anomaly at the bottom as a function of distance from site C1. (b) Propagation speed of the intrusion as computed from the arrival times (solid line) and as predicted from the ADCP velocity at 10 and 20 m above the bottom. The thick dashed line shows the theoretical gravity current propagation speed.

salinity sections along the approximately north-south lines depicted in Figure 2b from the CTD survey of 7–8 December 2009 show a region where isohalines from the upper level of the intrusion bow upward (Figure 10). This is most pronounced in the center portion of lines NS5 and NS6 but also over Cox Ledge at stations d37 and d47 of line NS7. The upward bowing of isohalines in these areas is suggestive of irreversible vertical mixing between the salty intrusion water and the fresher ambient water above.

The time series of moored salinity in Figure 6 indicate that depth-averaged salinity at all four sites increased by 0.5–1.0 over the approximate 3 week period during which the intrusion water was present (from 27 November just prior to the arrival of the intrusion at 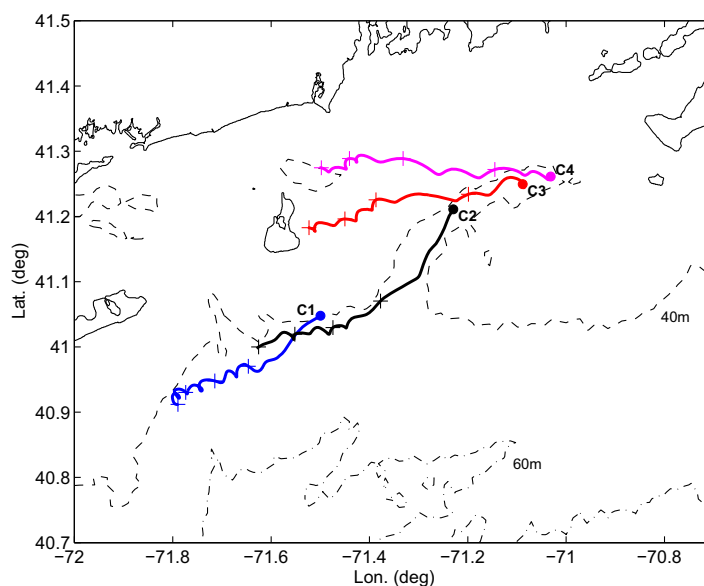C1 to 21 December). This increase is too large to be a manifestation of the seasonal increase in salinity occurring in winter in this region, which has been shown by *Ullman and Codiga* [2004] and *Codiga and Ullman* [2010] to be more on the order of 0.25. The observed increase in ambient salinity, above that expected from the seasonal cycle, in the RIS region is thus consistent with partial mixing of the high salinity intrusion with RIS waters.

4. Discussion

A lower bound on the spatial scale of the anomalous water mass can be estimated from the bottom temperature observations. Figure 7 shows that during the first intrusion period (late November–mid-December), there were instances in which temperatures in excess of 14°C, an approximately 2°C rise from preintrusion conditions, were observed simultaneously at all sites. The distance between sites C1 and C4 of 46 km thus represents a rough lower bound on the size of the feature.

We now address the question of the origin of the anomalous water mass. Previous hydrographic studies in the MAB have generally defined shelf water to be water with salinity <34 [*Mountain*, 1991; *Manning*, 1991; *Mountain*, 2003]. Shelf water is bounded on its offshore side by the shelfbreak front, which separates lower salinity shelf water from higher salinity water over the continental slope. The location of the shelfbreak front was defined by *Linder and Gawarkiewicz* [1998] as the 34.5 isohaline, which generally slopes upward in the offshelf direction. Thus, water with salinity of 35 must have originated on the offshore side of the shelfbreak front. In the shelfbreak front climatology of *Linder and Gawarkiewicz* [1998], for the region of the MAB from 69 to 72°W during late-autumn to early winter, the front intersects the bottom at approximately the 90 m isobath, roughly 85 km south of mooring C1.

The hydrography of the outer shelf south of New England was surveyed during early November 2009 as part of a NFSC cruise on the MAB shelf. Maps of near-bottom temperature and salinity from this cruise are shown in Figure 11 (the height above bottom for the near-bottom measurements ranged from 1 to 10 m). Although the warmest and saltiest water in the outer shelf CTD casts typically occurred near the bottom, in several instances highest temperature and salinity occurred above the bottom. In order to more definitively

Figure 9. Progressive vector diagrams (PVD) at 10 m above the bottom for 4 days before the first arrival of the intrusion at each bottom-mounted ADCP site. The different colors represent the PVDs for the different sites, with C1 in blue, C2 in black, C3 in red, and C4 in magenta. The plus signs along the psuedotrajectories are at 1 day intervals.

show the presence of intrusion water, the station symbols in Figure 11 are color coded to indicate the presence (black) or absence (white), at any depth in the CTD cast, of water with the approximate properties of the observed slope-water intrusion at C1 ($T \geq 15$ and $S \geq 34.5$). Slope water was observed on the shelf (water depths <100 m) at several stations east of 69°W between the 60 and 80 m isobaths on 10 and 11 November, at two stations at a longitude of approximately 69.75°W in water depths of 78 and 88 m on 4 November, and at one station in 92 m water depth at longitude of 70.7°W also on 4 November (Figure 11).

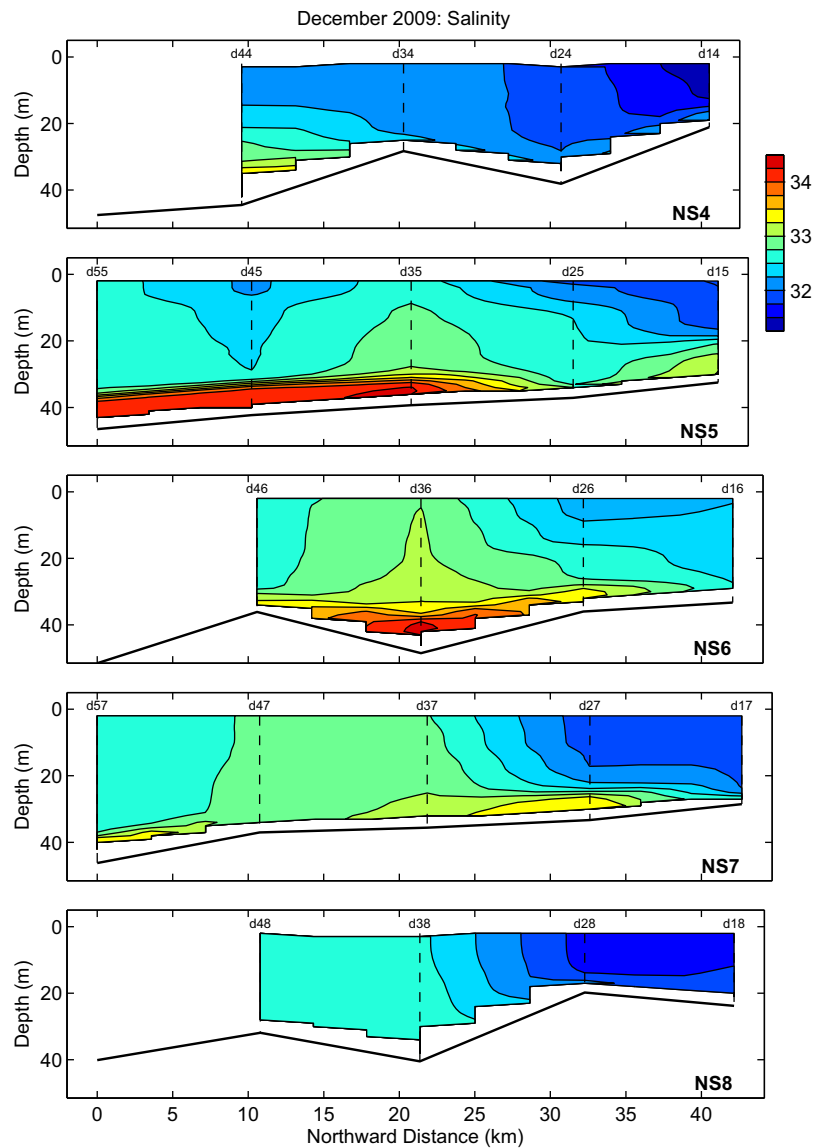To explain the presence of slope water on the shelf, we examined sea-surface temperature (SST) imagery of the shelfbreak region during November 2009. These data indicate the presence, in early to mid-November, of a Gulf Stream meander or warm core ring pressed up against the shelfbreak with its western edge at a longitude of about 68°W (Figure 12), or just east of the location of highest near-bottom T and S shown in Figure 11. A well-defined tongue of warm water extended westward from the meander along the continental slope and is suggestive of the warm streamers observed to the west of warm core rings by *Wei et al.* [2008]. The results of *Wei et al.* [2008] suggested significant onshelf flux of ring/slope water associated with the tongue. Model studies indicate the formation of a subsurface equatorward jet as well as cyclonic eddies within this tongue region with near-surface leakage onto the shelf [*Oey and Zhang*, 2004]. Although these studies suggest the possibility of direct ring-induced onshelf transport of slope/ring water, other studies show that the effect of rings can be more indirect. The surface front to the west of the ring in Figure 12 was located inshore of the 100 m isobath compared to its location well offshore of the 100 m isobath to the east of the ring interaction region suggesting that the ring has forced the shelfbreak front onshore. Interaction of rings with the front has been shown to increase the instability of the front [*Ramp et al.*, 1983; *Sloan*, 1996; *Morgan*, 1997] and there are suggestions in the literature that the resulting frontal eddies can enhance cross-frontal exchange [*Churchill et al.*, 1986; *Sloan*, 1996]. SST imagery from approximately 1 week later (not shown) shows evidence of intense frontal eddy activity, with spatial scales of roughly 50 km, along the front to the west of the ring. It thus seems quite likely that the near-bottom slope water observed on the outer shelf in the NOAA survey arrived there via either direct ring-induced onshelf transport or ring-enhanced shelfbreak eddy processes.

The progressive vector diagram in Figure 9 suggests that during the 4 days prior to its arrival, the leading edge of the intrusion approached C1 from the southwest. Since all the shelf CTD stations where slope water was observed during the November NOAA survey are located to the east and offshore of this inferred source area, the question that arises is what process brought the slope water to the vicinity of the 40 m isobath southwest of C1. The mean, near-bottom velocity components at C1 over the period from 4 to 28 November (0.004 m/s westward and 0.009 m/s northward) were far too low to transport a water parcel from the above-mentioned shelf CTD casts around 69.75°W near the 80 m isobath to C1. However, previous studies have shown that the mean along-shelf flow increases offshore over the southern New England shelf, with seasonal mean along-isobath currents during fall-winter at the 70 m isobath during the Coastal Mixing and Optics experiment in the range of 0.05–0.10 m/s westward [*Shearman and Lentz*, 2003]. Currents in this range would be sufficient to advect water westward from the 4 November CTD location (69.75°W at roughly

Figure 10. North-south vertical salinity sections from the CTD survey of 7–8 December 2009. The section names are denoted in the lower right of each plot. The locations of the sections are shown in Figure 2b. The positions of the CTD casts are indicated by the vertical dashed lines with station names above them.

the 80 m isobath) to a location due south of C1 on the 80 m isobath in 18–36 days, suggesting that along-isobath advection is a plausible explanation for the arrival of slope water southwest of C1 in late November. However, the cross-isobath movement of the intrusion cannot be explained either by observed cross-isobath currents at C1 during the period prior to the arrival of the intrusion, referred to above, or by the results of *Shearman and Lentz* [2003] who observed mean offshore currents on the outer shelf.

Although the actual size of the dense slope water mass observed in RIS is uncertain, the distance from its shelfbreak source suggests that it was likely an isolated water mass and not simply an onshore intrusion of the shelfbreak front. The behavior of isolated eddies on sloping shelves is thus relevant to the present discussion. Prior studies have examined the dynamics of lenses of dense water on sloping shelves and have shown the tendency for along-isobath propagation similar to the westward propagation of near-surface baroclinic eddies on a β-plane [e.g., *Nof*, 1983; *Mory et al.*, 1987; *Whitehead et al.*, 1990]. In the northern hemisphere, these eddies travel with shallower water on the right, which in the southern New England shelf case is westward. The theoretical propagation speed of a near-bottom lens with an infinitely deep and
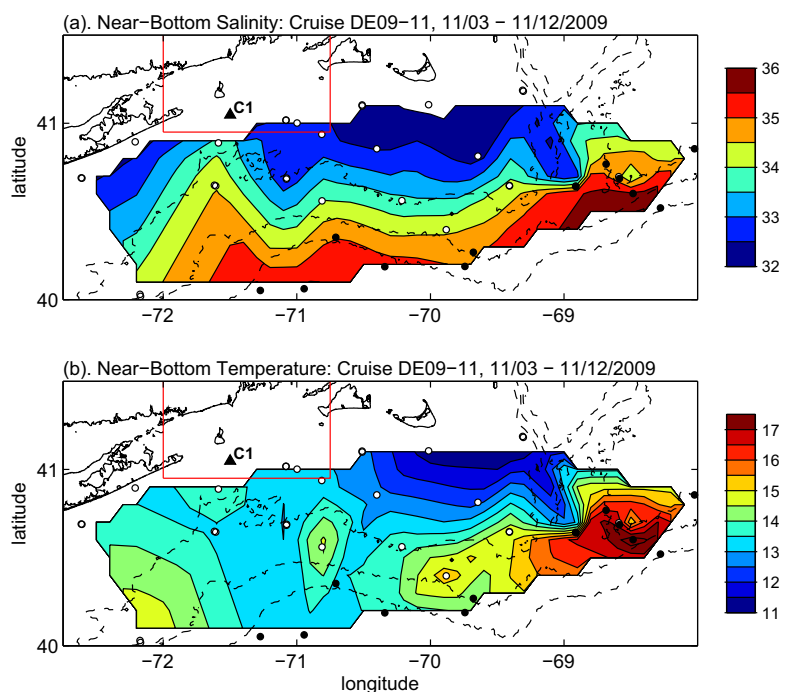
Figure 11. (a) Near-bottom salinity and (b) near-bottom temperature over the southern New England shelf during early November 2009 from CTD measurements made on NOAA Northeast Fisheries Science Center cruise DE09–11 aboard FSV *Delaware II*. The CTD cast locations are shown by the circles, with black-filled circles indicating stations where intrusion water ($T \geq 15$ and $S \geq 34.5$) was observed and white-filled circles where it was not. The dashed lines denote the 60, 80, and 100 m isobaths. The red rectangle shows the region covered by the survey maps of Figure 2. The black triangle indicates the location of mooring C1.

motionless upper layer is $C = \frac{g'S}{f}$ [*Nof*, 1983], where g' is the reduced gravity, S is the bottom slope, and f is the Coriolis parameter. Using a density difference of 1 kg/m³ between the intrusion water and ambient shelf water and a bottom slope of 10^{-3} gives a propagation speed of approximately 0.1 m/s, which is of the correct magnitude to explain the timing of the intrusion arrival at C1. It should be noted, however, that in laboratory experiments, the eddies are sometimes observed to propagate at a speed roughly equal to the theoretical value C [*Whitehead et al.*, 1990], while in other cases much slower propagation is observed [*Mory et al.*, 1987]. This is likely due to differences in the methods used to

generate the eddies. An important finding of *Mory et al.* [1987] is that the dense bottom eddies were observed to propagate into shallower water in addition to their along-isobath movement. The inferred onshore movement of the intrusion we observed, which cannot be easily explained, could possibly be due to such an effect.

The ecological significance of a near-bottom intrusion of slope water is likely dependent on the degree to which it mixes with the ambient shelf water. Slope water bel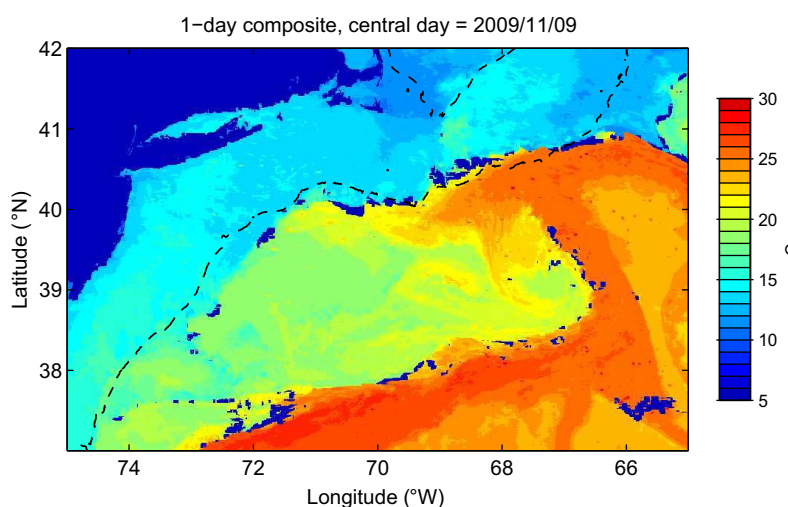ow the seasonal pycnocline is known to contain high concentrations of dissolved inorganic nutrients [e.g., *Hales et al.*, 2009], but if an intrusion of this water merely advances onshore and then retreats no net nutrient flux occurs. If, however, the intrusion mixes with the shelf water then an irreversible nutrient (and salt) flux has occurred. While we have no direct measurements of mixing in the RIS region, examination of the moored salinity time series in Figure 6 suggests that the 2009

Figure 12. Sea-surface temperature (SST) on 9 November 2009 from Advanced Very High Resolution Radiometer (AVHRR) satellite observations. All SST images from this date were combined using a warmest pixel composite method. The dashed line is the 100 m isobath.

intrusion did mix with the ambient shelf water. At all moorings, the salinity in late December is roughly 0.5–1 higher at all depths than the late-November salinity, prior to the onset of the intrusion. The intrusion period in 2009, as is generally typical of late fall to early winter conditions, was characterized by strong wind stress events and the associated velocity shears that could have driven the mixing of the intrusion waters. In fact, Figure 10 suggests the occurrence of at least localized mixing of the intrusion in RIS.

Although the analysis of the archived hydrocast data is definitive in suggesting that the fall 2009 slope water intrusion into the RIS region was a truly rare event, it is possible that the infrequent sampling of historical surveys might miss such a transient event. To determine whether a similar event occurred the following year, we examined moored CTD records from the late fall-winter of 2010–2011 at site C2 (Figure 1). The observations (not shown) did not show evidence of a similar intrusion during that winter. It is interesting to note, however, that *Gawarkiewicz et al.* [2012] present evidence of anomalously high bottom temperatures at water depths of 80–90 m south of New England during late fall 2011, which they attributed to the influence of the Gulf Stream, whose path at that time was much closer to the shelfbreak than normal. Unfortunately, no measurements in RIS are available from the 2011–2012 winter to ascertain whether the intrusion noted by *Gawarkiewicz et al.* [2012] penetrated as far inshore as the 2009 event.

5. Conclusions

The near-bottom intrusion observed in the RIS region during late autumn 2009 had salinity that was roughly 1 salinity unit higher than had ever been observed in the historical record in that region. The T/S properties of the intrusion clearly indicate that the water originated on the offshore side of the shelfbreak front. The spatial scale of the intrusion was estimated to be at least 45 km and it was present in the mooring region for 3–4 weeks, after which it appeared to retreat. The moored current observations indicate that an upwelling circulation due to strong eastward winds was responsible for the onshore movement of the intrusion from the southwest only during the final few days prior to its appearance in RIS. During the month preceding the intrusion, slope water with properties similar to the RIS intrusion was observed over the outer shelf southeast of RIS, likely due to the influence of a warm core ring interacting with the shelfbreak front. The available data do not allow a definitive identification of the process responsible for the transport of this water mass westward and onshore to the region southwest of RIS. From historical observations, the mean along-isobath current in that region is sufficient to advect the anomaly to RIS in the time required. However, it was also shown that the inferred speed was also consistent with the theoretical propagation speed of a dense bolus on the shelf. Although the fate of the autumn 2009 slope water intrusion is not known, the fact that it was observed nearly 100 km from the shelfbreak and that the moored salinity records indicated an increase in salinity over the intrusion time period suggests the likelihood that the intrusion did mix partially with ambient shelf water before it could retreat off the shelf. Such a process may represent a significant mechanism for the transport of salt and biogeochemical constituents across the shelf in the MAB.

References

Biscaye, P. E., C. N. Flagg, and P. G. Falkowski (1994), The Shelf Edge Exchange Processes experiment, SEEP-II: An introduction to hypotheses, results, and conclusions, *Deep Sea Res., Part II*, *41*, 231–252.

Boicourt, W. C., and P. W. Hacker (1976), Circulation on the Atlantic continental shelf of the United States, Cape May to Cape Hatteras, *Mem. Soc. R. Liege*, *10*, 187–200.

Boyer, T. P., et al. (2009), *World Ocean Database 2009, NOAA Atlas NESDIS 66*, 216 pp., U. S. Gov. Print. Off., Washington, D. C.

Churchill, J. H. (1985), Intrusions of outer shelf and slope water within the nearshore zone off Long Island, New York, *Limnol. Oceanogr.*, *30*, 972–986.

Churchill, J. H., P. C. Cornillon, and G. W. Milkowski (1986), A cyclonic eddy and shelf-slope water exchange associated with a Gulf Stream warm-core ring, *J. Geophys. Res.*, *91*, 9615–9623.

Churchill, J. H., J. P. Manning, and R. C. Beardsley (2003), Slope water intrusions onto Georges Bank, *J. Geophys. Res.*, *108*(C11), 8012, doi: 10.1029/2002JC001400.

Codiga, D. L., and D. S. Ullman (2010), Characterizing the physical oceanography of coastal waters off Rhode Island, Part 1: Literature review, available observations, and a representative model simulation, *Tech. Rep. 2*, Rhode Island Coastal Resour. Manage. Counc., Appendix to Rhode Island Ocean Special Area Management Plan, Wakefield, R. I. [Available at http://www.crmc.ri.gov/samp_ocean/finalapproved/TechRep02-PhysOcPart1-Codig aUllman2010.pdf.]

Garfield, N., and D. L. Evans (1987), Shelf water entrainment by Gulf Stream warm-core rings, *J. Geophys. Res.*, *92*, 13,003–13,012.

Gawarkiewicz, G. G., C. A. Linder, J. F. Lynch, A. E. Newhall, and J. J. Bisagni (1996), A surface-trapped intrusion of slope water onto the continental shelf in the mid-Atlantic bight, *Geophys. Res. Lett.*, *23*(25), 3763–3766.

Gawarkiewicz, G. G., R. E. Todd, A. J. Plueddemann, M. Andres, and J. P. Manning (2012), Direct interaction between the Gulf Stream and the shelfbreak south of New England, *Sci. Rep.*, *2*, 553, doi:10.1038/srep00553.

Gordon, A. L., and F. Aikman (1981), Salinity maximum in the pycnocline of the Middle Atlantic Bight, *Limnol. Oceanogr.*, *26*, 123–130.

Hales, B., R. D. Vaillancourt, L. Prieto, J. Marra, R. Houghton, and D. Hebert (2009), High-resolution surveys of the biogeochemistry of the New England shelfbreak front during summer, 2012, *J. Mar. Syst.*, *78*, 426–441.

Hare, J. A., and R. K. Cowen (1996), Transport mechanisms of larval and pelagic juvenile bluefish (*Pomatomus saltatrix*) from South Atlantic Bight spawning grounds to Middle Atlantic Bight nursery habitats, *Limnol. Oceanogr.*, *41*, 1264–1280.

Hopkins, J., J. Sharples, and J. M. Huthnance (2012), On-shelf transport of slope water lenses within the seasonal pycnocline, *Geophys. Res. Lett.*, *39*, L08604, doi:10.1029/2012GL051388.

Houghton, R. W., F. Aikman III, and H. W. Ou (1988), Shelf-slope frontal structure and cross-shelf exchange at the New England shelf-break, *Cont. Shelf Res.*, *8*, 687–710.

Legeckis, R., and T. Zhu (1997), Sea surface temperature from the GOES-8 geostationary satellite, *Bull. Am. Meteorol. Soc.*, *78*, 1971–1983.

Lentz, S., K. Shearman, S. Anderson, A. Plueddemann, and J. Edson (2003), Evolution of stratification over the New England shelf during the Coastal Mixing and Optics study, August 1996-June 1997, *J. Geophys. Res.*, *108*(C1), 3008, doi:10.1029/2001JC001121.

Lentz, S. J. (2003), A climatology of salty intrusions over the continental shelf from Georges Bank to Cape Hatteras, *J. Geophys. Res.*, *108*(C10), 3326, doi:10.1029/2003JC001859.

Linder, C. A., and G. Gawarkiewicz (1998), A climatology of the shelfbreak front in the Middle Atlantic Bight, *J. Geophys. Res.*, *103*, 18,405–18,423.

Manning, J. (1991), Middle Atlantic Bight salinity: Interannual variability, *Cont. Shelf Res.*, *11*, 123–137.

Morgan, D. (1997), Linear instability of the shelfbreak front off the southern flank of Georges Bank, PhD thesis, 190 pp., Dartmouth Coll., Hanover, N. H.

Mory, M., M. E. Stern, and R. W. Griffiths (1987), Coherent baroclinic eddies on a sloping bottom, *J. Fluid Mech.*, *183*, 45–62.

Mountain, D. G. (1991), The volume of shelf water in the Middle Atlantic Bight: Seasonal and interannual variability, 1977–1987, *Cont. Shelf Res.*, *11*, 251–267.

Mountain, D. G. (2003), Variability in the properties of shelf water in the Middle Atlantic Bight, 1977–1999, *J. Geophys. Res.*, *108*(C1), 3014, doi:10.1029/2001JC001044.

Nixon, S. W., et al. (1996), The fate of nitrogen and phosphorus at the land-sea margin of the North Atlantic Ocean, *Biogeochemistry*, *35*(1), 141–180.

Nof, D. (1983), The translation of isolated cold eddies on a sloping bottom, *Deep Sea Res., Part A*, *30*(2), 171–182.

Oey, L.-Y., and H. C. Zhang (2004), The generation of subsurface cyclones and jets through eddy-slope interaction, *Cont. Shelf Res.*, *24*, 2109–2131, doi:10.1016/j.csr.2004.07.007.

Ramp, S. R., R. C. Beardsley, and R. Legeckis (1983), An observation of frontal wave development on a shelf-slope/warm core ring front near the shelf break south of New England, *J. Phys. Oceanogr.*, *13*, 907–912.

Shearman, R. K., and S. J. Lentz (2003), Dynamics of mean and subtidal flow on the New England shelf, *J. Geophys. Res.*, *108*(C8), 3281, doi:10.1029/2003JC001972.

Shin, J. O., S. B. Dalziel, and P. F. Linden (2004), Gravity currents produced by lock exchange, *J. Fluid Mech.*, *521*, 1–34, doi:10.1017/S002211200400165X.

Sloan, N. Q., III (1996), Dynamics of a shelf-slope front: Process studies and data-driven simulations in the Middle Atlantic Bight, PhD thesis, 230 pp., Harvard Univ., Cambridge, Mass.

Ullman, D. S., and D. L. Codiga (2004), Seasonal variation of a coastal jet in the Long Island Sound outflow region based on HF radar and Doppler current observations, *J. Geophys. Res.*, *109*, C07S06, doi:10.1029/2002JC001660.

Ullman, D. S., and D. L. Codiga (2010), Characterizing the physical oceanography of coastal waters off Rhode Island, Part 2: New observations of water properties, currents, and waves, *Tech. Rep. 3*, Rhode Island Coastal Resour. Manage. Counc., Appendix to Rhode Island Ocean Special Area Management Plan, Wakefield, R. I. [Available at http://www.crmc.ri.gov/samp_ocean/finalapproved/TechRep03-PhysOcPart2-Ullma nCodiga2010.pdf.]

Wei, J., and D.-P. Wang (2009), A three-dimensional model study of warm core ring interaction with continental shelf and slope, *Cont. Shelf Res.*, *29*, 1635–1642, doi:10.1016/j.csr.2009.05.009.

Wei, J., D.-P. Wang, and C. N. Flagg (2008), Mapping Gulf Stream warm core rings from shipboard ADCP transects of the Oleander Project, *J. Geophys. Res.*, *113*, C10021, doi:10.1029/2007JC004694.

Whitehead, J. A., M. E. Stern, G. R. Flierl, and B. A. Klinger (1990), Experimental observations of baroclinic eddies on a sloping bottom, *J. Geophys. Res.*, *95*(C6), 9585–9610.

Wright, W. R. (1976), The limits of shelf water south of Cape Cod, 1941 to 1972, *J. Mar. Res.*, *34*, 1–14.

Wright, W. R., and C. E. Parker (1976), A volumetric temperature/salinity census for the Middle Atlantic Bight, *Limnol. Oceanogr.*, *21*, 563–571.